Distribution Agreement

In presenting this thesis as a partial fulfillment of the requirements for a degree from Emory University, I hereby grant to Emory University and its agents the non-exclusive license to archive, make accessible, and display my thesis or dissertation in whole or in part in all forms of media, now or hereafter known, including display on the World Wide Web. I understand that I may select some access restrictions as part of the online submission of this thesis. I retain all ownership rights to the copyright of the thesis. I also retain the right to use in future works (such as articles or books) all or part of this thesis.

Nandish Vora April 10, 2023

Bridging the Gap: New Physics in Confined Droplet Coalescence

by

Nandish Vora

Justin Clifford Burton
Adviser

Physics

Justin Clifford Burton
Adviser

Daniel Sussman
Committee Member

Yiran Wang
Committee Member

2023

Bridging the Gap: New Physics in Confined Droplet Coalescence

By

Nandish Vora

Justin Clifford Burton
Adviser

An abstract of
a thesis submitted to the Faculty of the Emory College of Arts and Sciences
of Emory University in partial fulfillment
of the requirements for the degree of
Bachelor of Science with Honors

Physics

2023

Abstract

Bridging the Gap: New Physics in Confined Droplet Coalescence
By Nandish Vora

Coalescence is the process via which two droplets merge and become one through the formation of a "bridge" or "neck" between them which is driven by Laplace pressure. Coalescence of simple fluids in various different experimental situations has been a long studied problem with various applications in very pertinent fields. However, recently there has been a push for furthering our understanding coalescence of more than just fluids. Particular of interest is biological aggregates and colloidal systems where dissipation plays a large role. It is understood that a governing law that can describe such systems is given by Darcy's Law, a mathematical model describing fluid flow through porous materials. In this experiment we use confined droplet coalescence to understand how these systems work and what the characteristics of coalescence are. We show what the necessary conditions are to test Darcy coalescence and what an experiment might look like. Our experiments have shown that the neck width grows as a power law in time with a power of ~ 0.4 during coalescence. Furthermore, our work emphasizes the challenges involved in building an experimental set up that truly imitates the aggregate systems we are trying to understand.

Bridging the Gap: New Physics in Confined Droplet Coalescence

by

Nandish Vora

Adviser: Justin Clifford Burton

A thesis submitted to the Faculty of the Emory College of Arts and Sciences
of Emory University in partial fulfillment
of the requirements for the degree of
Bachelor of Science with Honors

Physics

2023

Acknowledgments

I gratefully acknowledge Dr. Daniel Sussman and Dr. Yiran Wang for taking time out of their schedules to serve on my committee. I thank Dr. Justin Burton and the rest of BurtonLab who have been phenomenal mentors and a support system in my last two years in the lab. None of this would be possible without them. Dr. Burton gave me the opportunity to start research as a second year and without his mentoring, support, and friendship, I would not be where I am. Lastly, I would like to thank my friends and family. I am lucky and grateful for the community I have found at Emory and this was reinforced when I had 10 of my lovely friends wake up early on a Monday to attend my defence. Without their support, I would not be where I am and certainly would not have been able to do good job.

Contents

List of Figures

Chapter 1

Introduction

1.1 What is coalescence?

During coalescence, two fluid droplets merge through the formation of a liquid bridge which reduces the interfacial energy between the two droplets. This bridge is then driven by surface tension and expands. The dynamics of this phenomenon are controlled by Laplace pressure and starts out of a singularity forming due to infinite curvature of the bridge at the point of contact. This singularity and the formation of the bridge has been studied when the coalescence takes place in air or in vacuum [5]. Most experimental works study the growth of the neck radius $r(t)$ as a function of time. After plenty of work on the problem, the current understanding is that when two droplets are brought into contact, the initial dynamics are governed by inertial and viscous forces [6]. Yet for small droplets, inertial forces are negligible and the system is in Stokes flow [7]. Once in the Stokes regime, the dynamics can be described by an analytical solution for the droplet shape evolution [8, 9, 10].

1.2 Applications of coalescence

Coalescence falls under the class of free surface problems with plenty of importance in different areas some which are discussed here. In the food industry [11, 12], production of food products involves mixing of liquids. Stabilising these mixtures is essential to maintain shelf life and taste, and is rooted in the coalescence processes. Further, Stability of emulsions and suspensions are affected by coalescence and mixing problems [13, 14, 15, 16]. In the petroleum industry [17], coalescence of oil drops and its interaction with surrounding solutions is important. Understanding the dynamics of coalescence would be important to streamline oil clean up and separation techniques. In the field of meteorology, coalescence of cloud and rain droplets is important to understand the development of weather patterns and predicting weather phenomena [18]. In medicine, understanding the coalescence of blood cells in clotting processes or detecting tissue defects is rooted in understanding coalescence [19]

Based on past work, we can analyse characteristics of coalescence processes such as the scaling law for bridge width $r(t)$, the curvatures of the bridge, and the overall shape of the droplets to characterise and understand the physics of the initial moments of coalescence and the ensuing dynamics.

1.3 New age of coalescence problems

In recent years, coalescence is being studied under a new lens. It is used as the basis to study and understand the dynamics of liquid-like systems such as biological aggregates. Critical living systems processes like cancer invasion and tissue engineering can be better understood by learning about the fusion dynamics of these liquid-like systems [19, 20, 21].

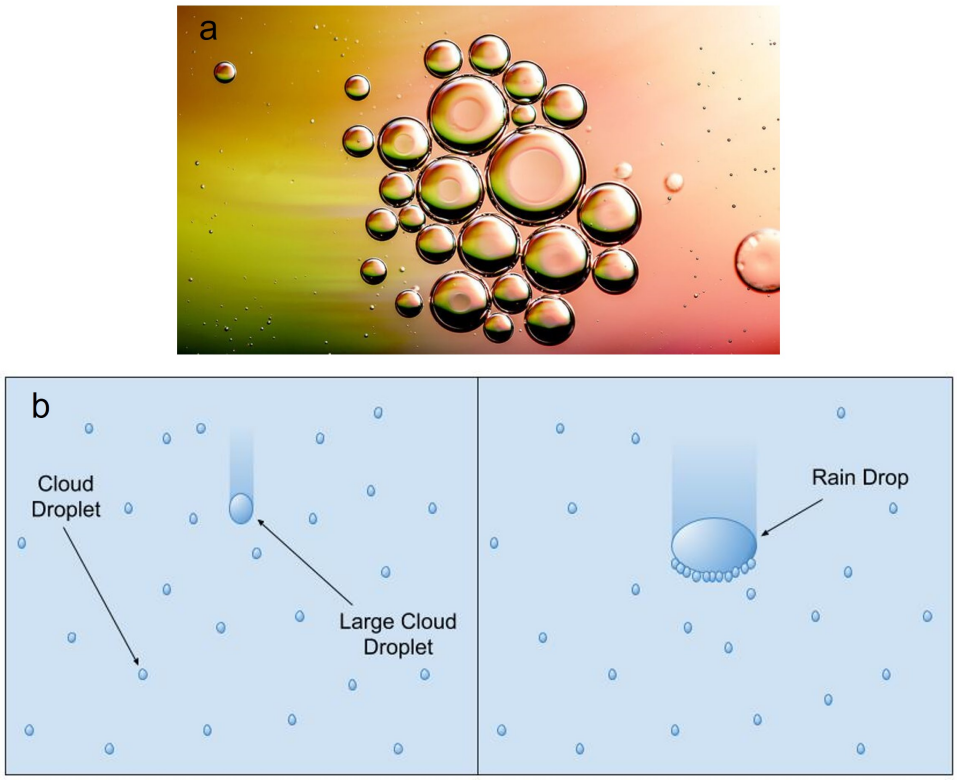

Figure 1.1: a) Application of coalescence to understanding how oil droplets coalesce to improve oil extraction and spill clean up efforts [1] b) Application of coalescence in meteorolgy and rain drop formation from cloud droplets Courtesy: Atmospheric Processes and Phenomena, Press Books

Most of these systems exist at a low Reynold's number. Coalescence is understood well for such a system with simple liquids. However, more complex systems like colloidal structures, polymers, and aggregates of living matter are not well understood. Additional complexities are added to our understanding of simple liquid coalescence models, such as friction or, viscoelatsic terms to explain differences from well understood models and characteristics like scaling laws [22]. A particular application of understanding these new coalescence problems is the measurement of quantities like surface tension in systems where these quantities are hard to measure as is in the case of the coalescence of cell nucleoli [23].

In a more recent work done by Yue et. al. [2], they show that in these complex

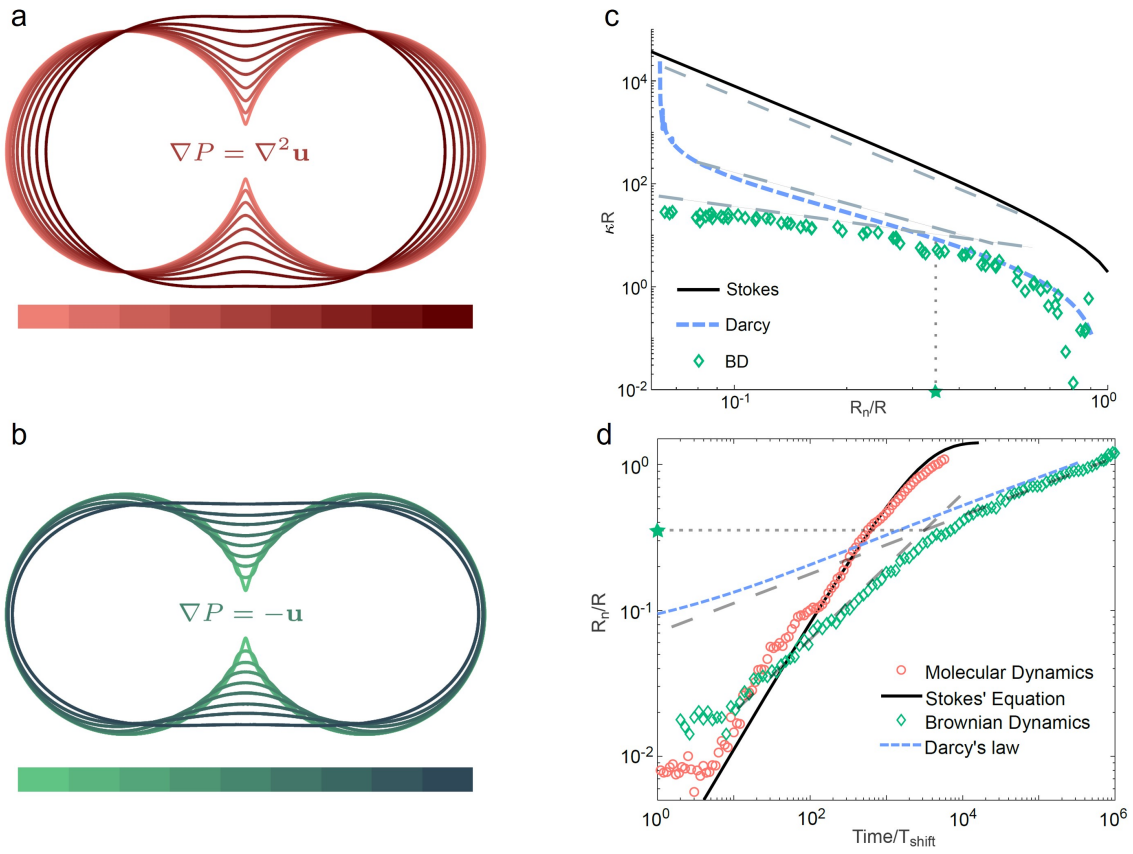

Figure 1.2: a) Simulations done to show what the overall shape of coalescence looks like when fluid flow is governed by Stokes equation. b) Simulated overall shape when fluid flow is governed by Darcy flow (Darker colors are later in time). c) Results from simulations showing how curvatures scale in coalescence in various regimes. Dashed grey lines have a slope of -2 and -3 to guide the eye. d) Results from simulations showing how the neck width scales in time. Dashed grey lines have slope 1/2 and 1/5 to guide the eye. Taken from the work by Yue et. al. [2]

systems coalescence is coupled to a viscous, dissipative background. Such systems can be understood better by adding frictional terms to the Navier-Stokes description. They draw the comparison to using Brownian Dynamics rather than Molecular Dynamics to model systems at a molecular level. They link this new continuum model to Darcy's Law, a mathematical description of fluid flow through a porous medium given by:

$$-\boldsymbol{\nabla} P = \alpha \mathbf{v} \tag{1.1}$$

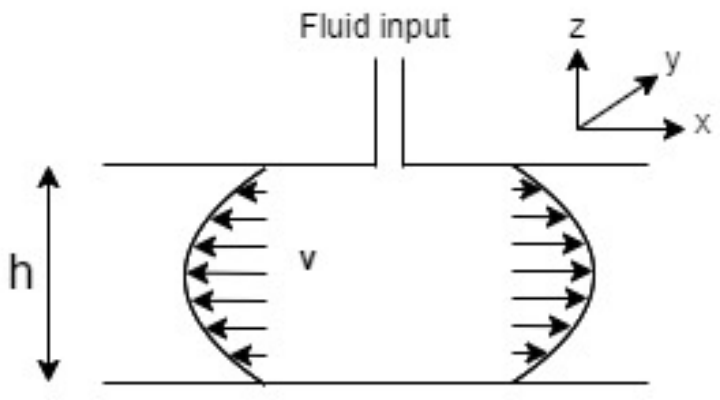

Figure 1.3: Poiseulle flow between two parallel plates in a Hele-Shaw cell

where α is a proportionality constant.

Yue et. al. expand upon how this changes the characteristics of droplet coalescence such as the overall shape of the droplets and the time dependence of the growth of the neck. Fig. 1.2 a) and b) shows the difference in the overall shape of coalescence between Stokes flow and Darcy flow. In Darcy flow you can see that the two individual droplets are not really drawn to each other but the neck still grows creating a sort of oval race track shape. Fig. 1.2 c) shows that under Darcy flow, Yue et. al. think that the curvature of the neck goes as R/r^2 as opposed to R^2/r^3 in the usual Stokes regime case. Fig. 1.2 d) shows that the neck width scales as a power law $r \propto t^\beta$ where $\beta = 1/5$ at late times. However, in these simulations at early times, the curvature is cut off by a particle size leading to what looks like a power law with $\beta = 1/2$

Our experiments arise from aiming to understand the scaling law that governs the growth of the coalescence neck and compare it to results obtained from simulations.

1.4 Studying Darcy's Law using a Hele-Shaw cell

To test how coalescence takes place under Darcy's Law, we need a technique to make Darcy's Law the governing law for fluid motion. One way to do this is by coalescing our droplets in a Hele-Shaw cell where the Darcy flow governs fluid dynamics. We assume viscous and incompressible flow between two parallel plates a distance h apart. We can then assume that the flow in this region is Posueille flow and must be parabolic in the z direction as shown in Fig. 1.3. Further we say that the flow depends only on the x-position. We take the average velocity between the plates with Posueille flow

$$\mathbf{v} = \frac{6}{h^2} z(h-z)\langle v_x(x,t), v_y(x,t), 0\rangle \tag{1.2}$$

The prefactor of $\frac{6}{h^2}$ can be determined by taking the expression $z(h-z)\langle v_x(x,t), v_y(x,t), 0\rangle$ and averaging over the gap size. We know that the flow is in the Stokes regime and we can use Stokes equation $\boldsymbol{\nabla} P(x,y) - \eta \boldsymbol{\nabla^2} \mathbf{v}(x,y,z) = \mathbf{0}$. Plugging our velocity into this equation we get

$$\left\langle \frac{\partial P}{\partial x} - \eta\left(-\frac{12 v_x(x,t)}{h^2} + \frac{6(h-z)}{h^2}\frac{\partial^2 v_x}{\partial x^2}\right), \frac{\partial P}{\partial y} - \eta\left(-\frac{12 v_y(x,t)}{h^2} + \frac{6(h-z)}{h^2}\frac{\partial^2 v_y}{\partial x^2}\right), 0 \right\rangle = \mathbf{0} \tag{1.3}$$

We can integrate equation (1.4) across the gap size to get rid of the z dependence and we end up with

$$\left\langle \frac{12\eta}{h^2} v_x(x,t) + \frac{\partial P}{\partial x} - \eta\frac{\partial^2 v_x}{\partial x^2}, \frac{12\eta}{h^2} v_y(x,t) + \frac{\partial P}{\partial y} - \eta\frac{\partial^2 v_y}{\partial x^2}, 0 \right\rangle = \mathbf{0} \tag{1.4}$$

We are left with some extra terms. If we compare $\frac{v_x}{h^2}$ with $\frac{\partial^2 v_x}{\partial x^2}$ (and the same for the y terms), we can assume that the former is a much larger term as the gap thickness h tends to zero. This basically means that length scales in the x and y-directions, are

much larger than h, So, let's set these terms to zero. Hence we end up with:

$$-\frac{h^2}{12\eta}\boldsymbol{\nabla} P = \mathbf{v} \tag{1.5}$$

Equation (1.6) is Darcy's Law. The assumptions we have made here are that:

1. The gap size is small. Which means the inertial terms can be neglected and the Reynold's number is low.

2. Gradients in the flows in the xy-direction are at a larger scale than the gap size, h and hence they can be neglected.

1.5 Coalescence in a Hele-Shaw Cell

There are a few investigations that outline the coalescence of fluids in a Hele-Shaw cell and its characteristics. In Ref. [4], they use a vertical Hele-Shaw cell to study the coalescence of a drop as it falls into a bath of the fluid, i.e. gravity drives the drop toward the fluid until they coalesce. It must be noted that this is not coalescence of two drops, but the coalescence of a drop on a planar interface; but we do not think this makes a difference. This is varied for two gap sizes and various drop radii. They report on the time scaling law for the growth of the neck as $r \propto t$ in early times which crosses over to $r \propto t^{1/4}$ at later times. This is followed up with a mathematical work [24] where they show why the scaling law must follow a 1/4 power law. However, we do not understand how they have accounted for effects of gravity. Further, their analysis of the scaling does not arise out of a Darcy's Law argument.

In another work Ref. [3], they coalesce nematic droplets within an isotropic fluid. The gap size was kept constant at $5\mu m$ and coalescence was investigated for various drop sizes. The scaling law of the neck growth was reported as a 1/4 power law. In

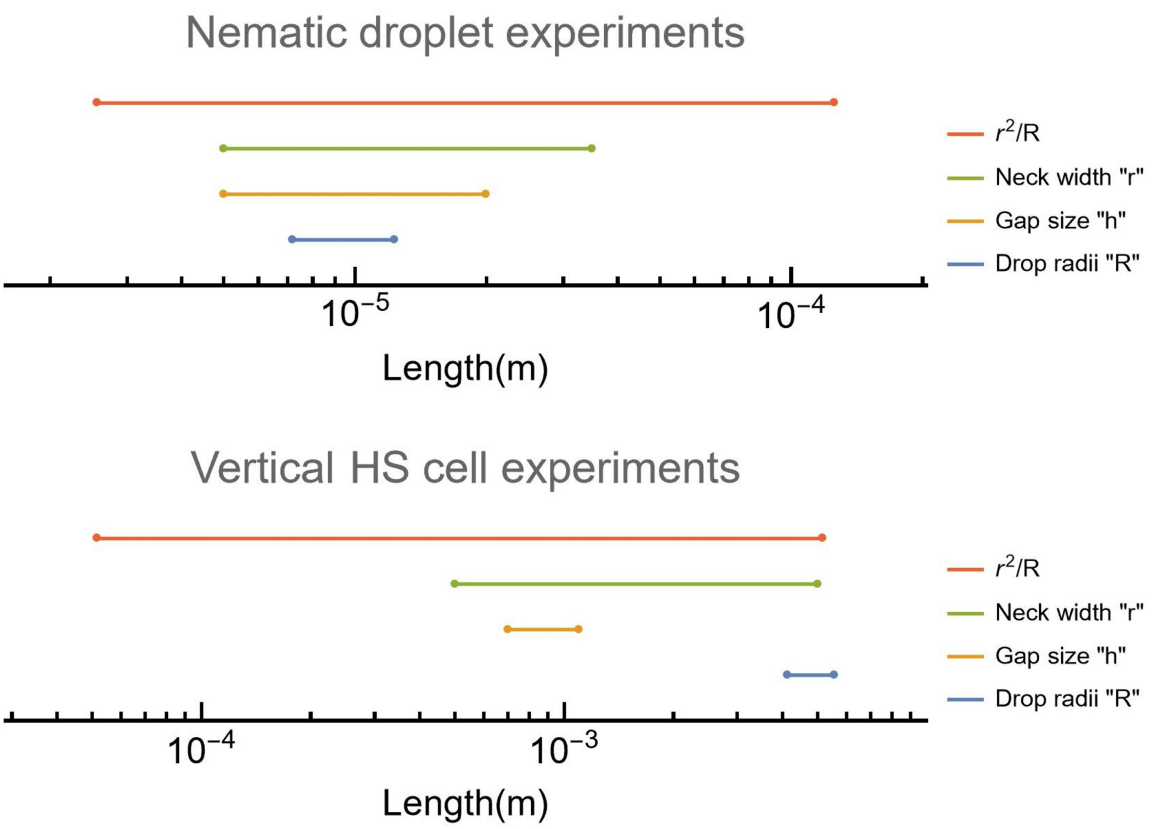

Figure 1.4: Length scale comparison for experiments done in coalescence of nematic-isotropic fluids in a Hele-Shaw cell (top [3]) and in a vertical Hele-Shaw cell (bottom [4]. The lengths are plotted on a log scale and the measurement scale is indicated in the titles.

this case also, there is no analysis of scaling from a Darcy's Law perspective.

In both cases, the scaling law is promising and agrees to a certain extent with the analysis done in Ref. [2]. However, we note that neither of these experiments, even though conducted in a Hele-Shaw cell, may not be in the regime where Darcy flow is the governing law.

We did an analysis of the various parameters of their experiments like the gap sizes (h), drop radii (R), and the neck width (r). Flow is determined by curvature such that the flow is over the length scale associated with the curvature. As shown

in 1.2 [2] the curvature of the neck is roughly given by the quantity R/r^2 This means that the length it is associated with is r^2/R. When we compare all these length scales to the gap size, we note that the gap size is not the smallest length scale in the experiment, in fact the neck widths and drop sizes are comparable to the gap size which violates our assumptions made for Darcy's Law. In the derivation of Darcy Flow being the governing law in a Hele-Shaw cell, we think that h should be much smaller than any other length scale in the problem in order to ignore higher order derivatives. However, if the length scale at which those derivatives matter are smaller or comparable to the gap size, we can no longer ignore flows at that scale. Hence, this is not in a pure Darcy Law case, but some in-between. These length scale comparisons are plotted on a log number line as shown in Fig. 1.4.

Hence, in order to truly test Darcy coalescence, the experiment must have the gap size as the smallest scale. And as we will show with our experiments, this is difficult to achieve. However, in our experiments we are able to ensure that the drop radii are much larger than the neck width which in turn is much larger than the gap sizes.

Chapter 2

Methods

2.1 Experimental Set Up

In our experiment, we aimed to simultaneously grow two quasi-2D cylinders (disks) of equal radii and then coalesce them.

To do this, we designed to acyrlic circular plates of diameter 15 cm, each. We fitted the upper plate with two holes spaced 6 cm apart. We used 1.5 mm NPT barbed fittings to inject fluid into the cell via the two holes. We then connected the NPT fittings to a syringe using a 1.5 mm rubber tubing. We then employ a syringe pump to inject fluid a constant volume rate.

The two plates of the calla are separated using plastic shims of widths 100 μm, 250 μm, and 500 μm, which is the gap size, h.

Initially, we attempted to use a mixture of glycerol and water as our fluid. However, we faced many difficulties in growing perfect disks and were unable to achieve a consistent mix to standardise the viscosity. We would have had to employ humidity control measures in order to fix the viscosity since a glycerol-water mix can absorb

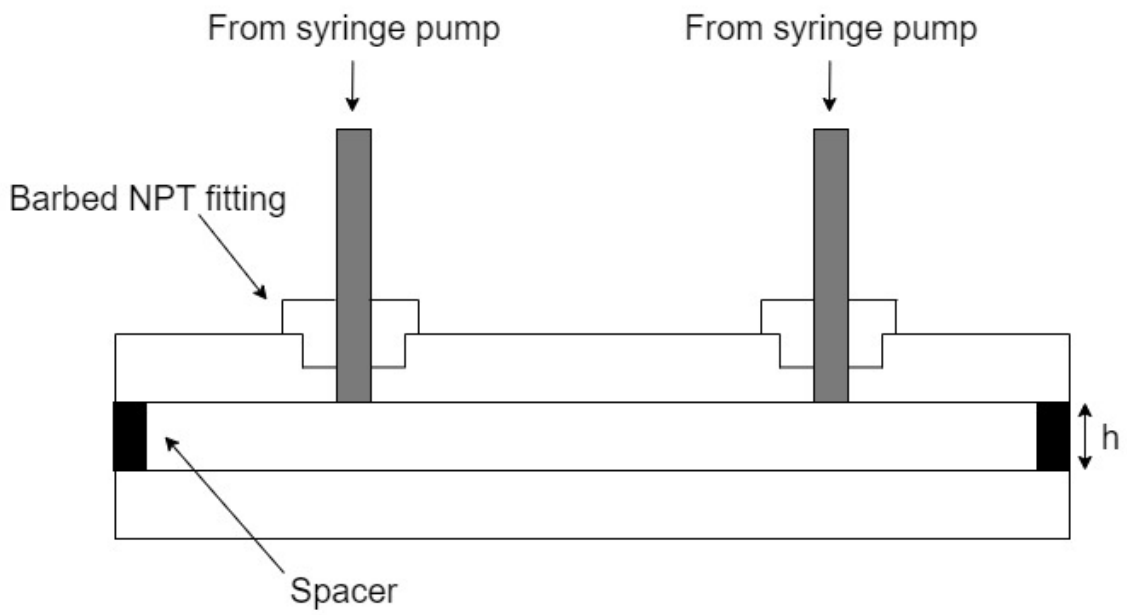

Figure 2.1: Experimental set up

humidity and change its nature. Further, we linked the imperfect disks to an issue of pushing contact lines on the acrylic sheet. We tried addressing this issue by pumping the entire cell with high density silicone oil before injecting just glycerol. However, we inadvertently caused the growth of fingers due to viscous effects. We noticed that when we were pumping the silicone oil into the cell, it grew out in nearly perfect disks. After trials and errors, we settles on using 200 cSt Si oil as our fluid. Further, to improve the smoothness of the contact lines, we waxed the acrylic plates with Rain-X fluid repellent. This allowed us to grow perfect disks of radii $\approx$ 3 cm and then coalesce them.

2.2 Preparation and Execution

Before each experiment, we washed both acrylic plates with water and soap and dried them thoroughly. We then waxed each plate with multiple uniform coats of Rain-X fluid repellent. We then placed the shims to separate the plates by the desired gap size, h and secured the set up using large clips such that the plates are squeezed onto

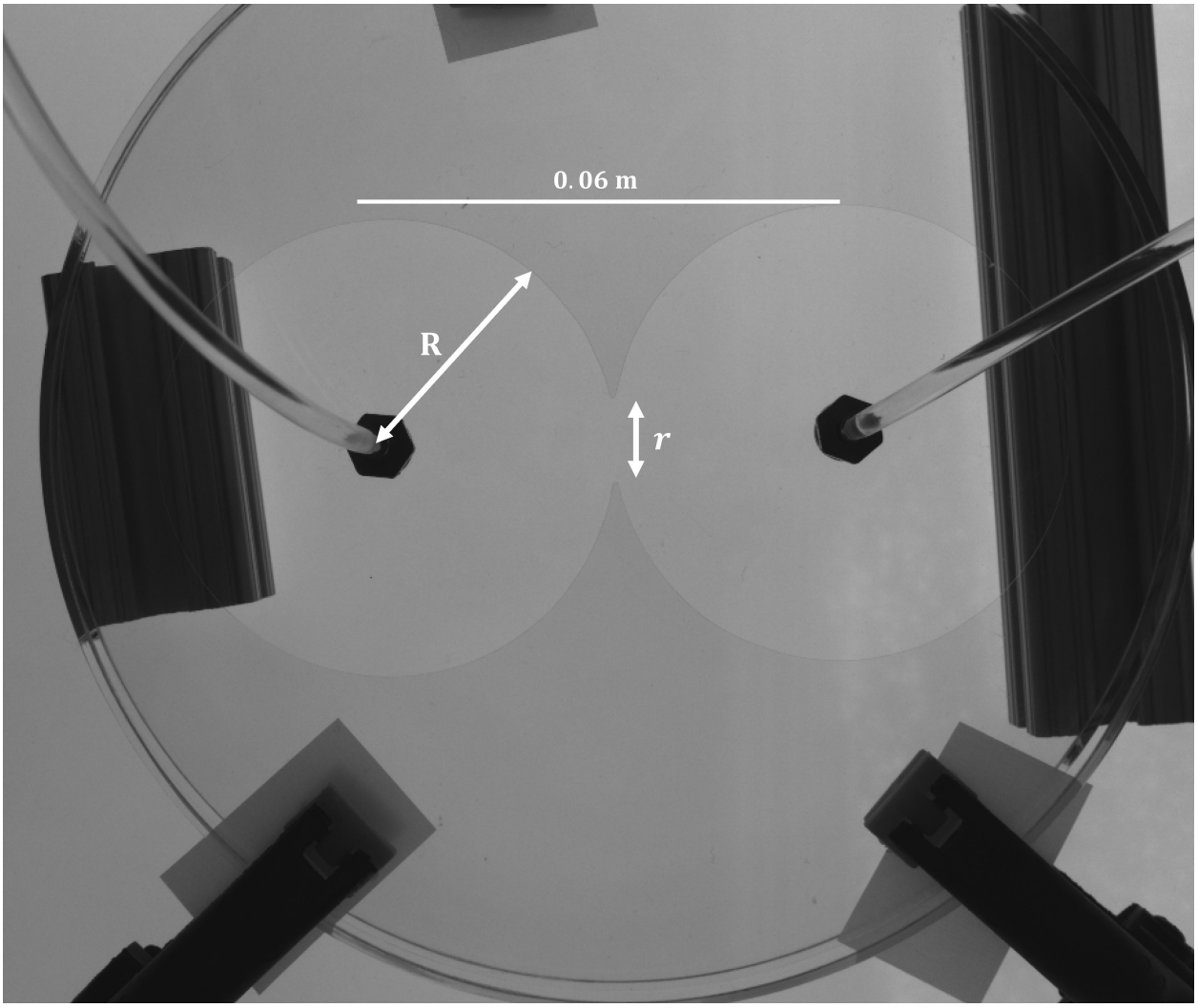

Figure 2.2: Picture of a frame from an experiment with gap size 100 μm

the shims and they do not move. This is now a Hele-Shaw cell. The cell is placed on top of an LED light for illumination. We then plug in the rubber tubing into the NPT fittings attached to the syringes of Si oil.

At this point, we start pumping the fluid in at a constant volume rate depending on what the gap size is. We pump at 0.1 ml/hr, 0.25 ml/hr, and 0.5 ml/hr for the respective gap sizes; 100 μm, 250 μm, and 500 μm. Both pumps are turned on simultaneously so that the drops grow together and coalesce when they are roughly

the same size. The injection points were designed to ensure this. Once the droplets are very close, we turn off the pump so that no more fluid enters the system and the coalescence is not affected by the constant influx of volume. This is further discussed in section 2.3.

Once the pumps are turned off, we record the coalescence from above using a high-speed Point Grey camera at 70 fps. We record the coalescence for roughly 10 seconds to capture earliest behaviour and some late behaviour. The images are then processed using ImageJ software and exported to Tracker software in video format. We then manually click off points for the two edges of the neck and calculate the distance between them as the two ends of the neck grow apart during coalescence. Figure 2.2 shows an image from an experiment.

We then analyse this data in Wolfram Mathematica to understand the scaling law for the neck growth.

2.3 Growing a drop with a constant volume injection

We briefly mentioned the effect of pumping in the fluid in our experiment. It is important to understand how the disk grows in the Hele-Shaw cell and how pumping will effect the coalescence process. We first understand how the disk grows in the cell.

Lets look at the the function that describes the radius of a quasi-2D cylinder as it grows under constant volume input in a Hele-Shaw cell. Let the volumetric rate $V'(t) = k$. We also know from basic geometry that $V'(t) = 2\pi hr(t)r'(t)$. Hence we

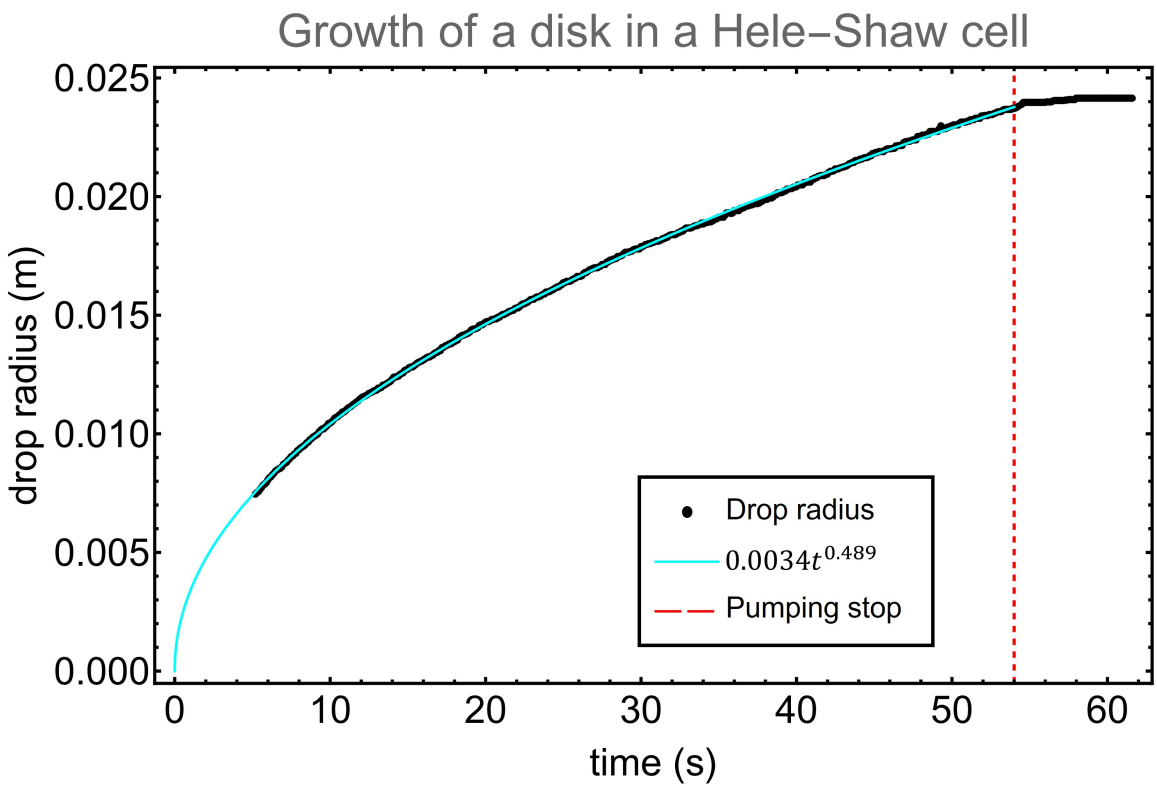

Figure 2.3: Radius of drop measured as it grows in a Hele-Shaw cell with constant volume injection for a gap size of 250 microns. The fitted power is 0.489 ± 0.001

solve the following differential equation:

$$2\pi h r(t) r'(t) = k \tag{2.1}$$

with the initial conditions

$$r(0) = 0 \tag{2.2}$$

Using separation of variables we can find the solution for $r(t)$:

$$r(t) = \sqrt{\frac{kt}{\pi h}} \tag{2.3}$$

Hence, we should see the growth of the disk go as $t^{1/2}$. We can also predict the prefactor $\sqrt{\frac{k}{h\pi}}$.

Our volume rate, $k = 6.5 \times 10^{-9}\ m^3/s$ and the gap size , $h = 250 \times 10^{-6}\ m$. Hence, we predict a prefactor of 0.0029

We conduct a test run to confirm this and to also understand if and how the drop continues to grow once the pump is turned off. Fig. 2.3 shows that we see the 1/2 power law growth and the growth comes to a stop after a small transient once the pump has been turned off. This confirms that once the pumps are turned off, the drops are barely growing anymore and the coalescence we are concerned with is not being affected by pumping.

Chapter 3

Results and Discussion

3.1 What we see

The initial coalescence is very rapid and you can see the quick formation and growth of the neck. At the point of contact, the curvatures are very high as you can see in the first image of Fig. 3.1. Recall that the pumps have been stopped before the coalescence process even started, so there is no new fluid being added to the system as the neck grows. Eventually, we see that the neck growth gets arrested and the neck radius does not increase further. You can see this in Fig. 3.2. We think this is because there is no pump to provide enough pressure to overcome and drive the contact line in the Hele-Shaw cell. Sometimes contact lines can get pinned for various reasons such as particle-particle interactions, colloids attaching to interfaces, or polymer chains getting stuck in interfaces etc. [25]. An example would be a water droplet pinning to a car windshield. So, we can divide what we see in our experiment into two regimes; the initial growth phase, and the slow-down arresting phase.

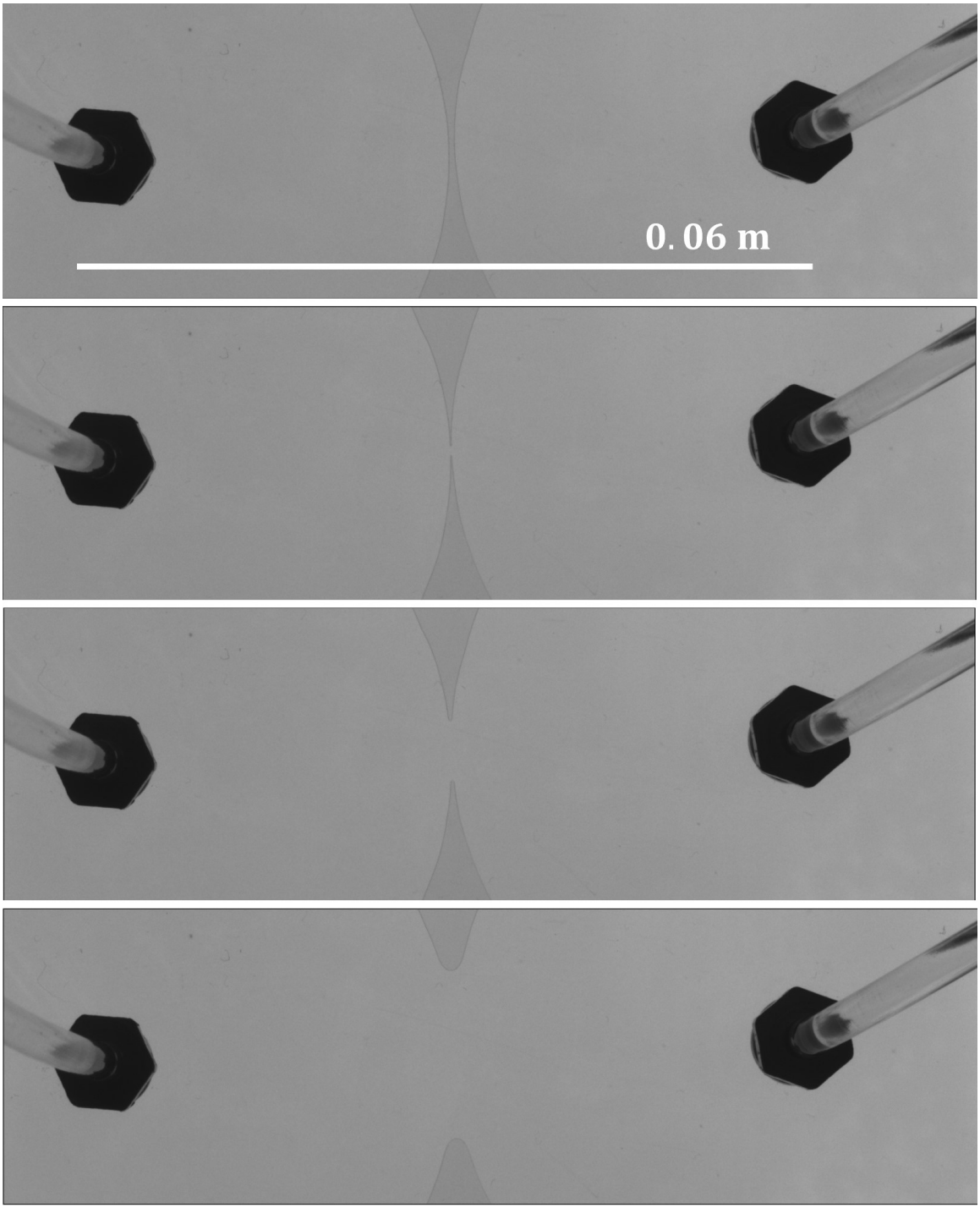

Figure 3.1: Sequence of images of the coalescence process. Let t_0 be the time at which coalscence occurs. The frames are captured at the times as follows: $t_0 - 1$ s, $t_0 + 0.1$ s, $t_0 + 5$ s, and $t_0 + 90$ s. You can see evolution from a sharp curvature at the beginning to a shallow curvature when the coalescence arrests after a slow down.

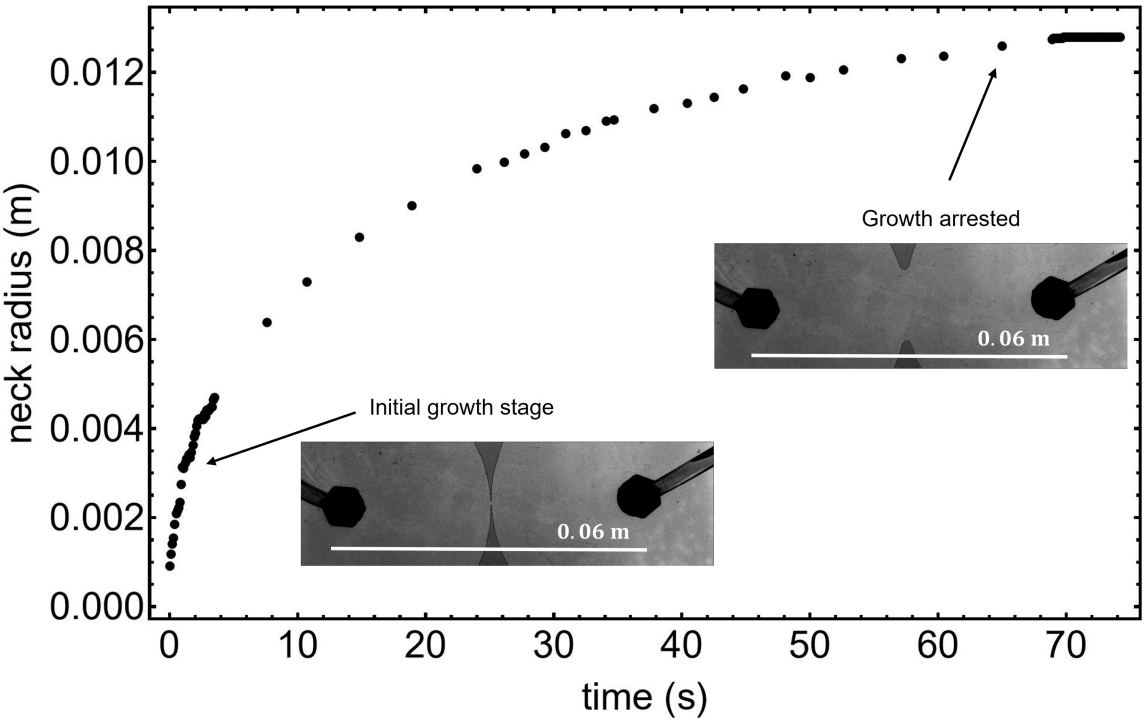

Figure 3.2: Coalescence gets arrested after some time due to not enough pressure in the system to push the contact line

3.2 Time dependence of bridge growth

We are now at a position where we can analyse the growth of the neck as a function of time. We plot the neck width in time for the various gap sizes we tested. In all cases, the drop radii are ≈ 3 cm. Fig. 3.3 shows this raw data. Each data set was fitted to an equation of the form of

$$r(t) = a(t - t_0)^{\tau} \tag{3.1}$$

We shifted each data set such that t_0 was negligible so that every data set starts from near zero. After fitting, we plotted each function with the data. We expect the gap size to affect the rate of growth based on Eq.(1.7) and also affect the gradients in pressure.

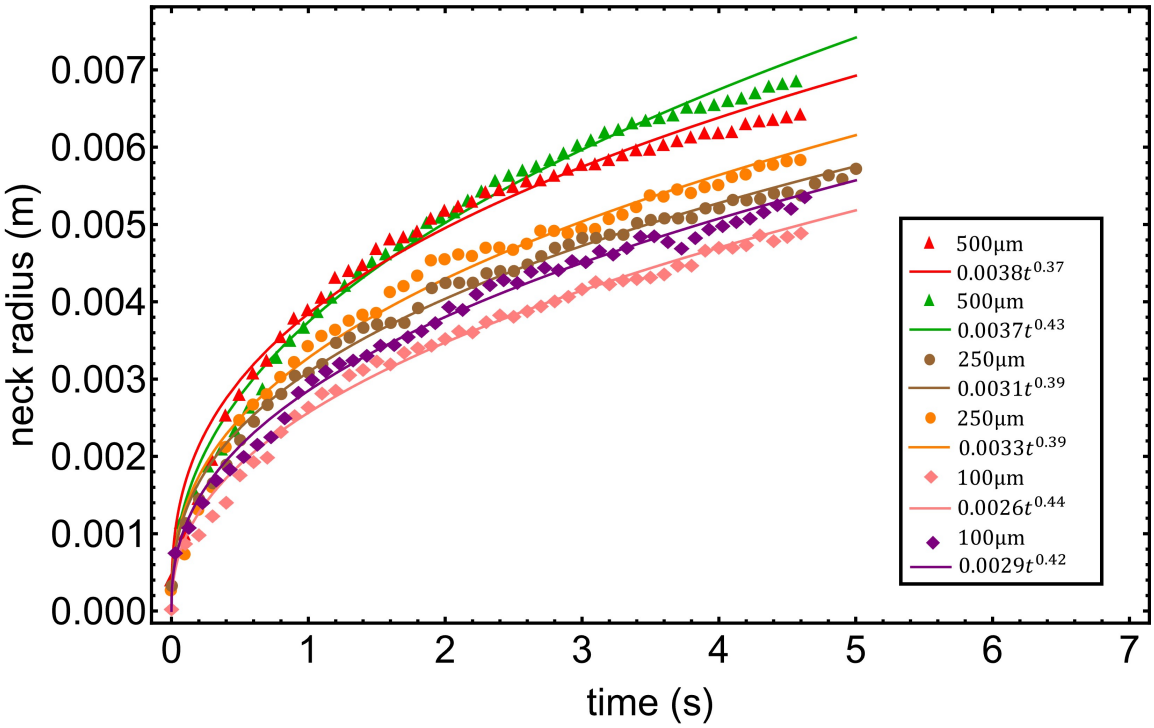

Figure 3.3: Neck width plotted as a funtion of time along with the power law fits fitted using Eq.(3.1)

Fig. 3.3 shows data from our experiments with three different gap sizes. We can see that the fastest coalescence takes place for the largest gap size and then we go in decreasing order. However, we expect the different between the velocities to go $\propto h^2$. However, we think that there are more nuances involved in this since the pressure gradients involved also depend on h. We in fact do not see a large enough difference like we would if it only depended on h^2. Further, based on the various fits we can see that we fit our data with a power law and the power on average is 0.39 ± 0.02. There are some inconsistencies in the fits and the there might be more than meets the eye with the functional form this data follows. However, a lot more can be revealed if we plot this on a log-log plot.

We can non-dimensionalise the data points with pre-factors. We chose the $\frac{\gamma}{\eta R}$ as the scaling for time, and $\frac{1}{h^{1/5}R^{4/5}}$ for scaling the neck width. We plot this on a log-log plot in Fig.3.4 and see a somewhat collapse of data. We wanted to compare the

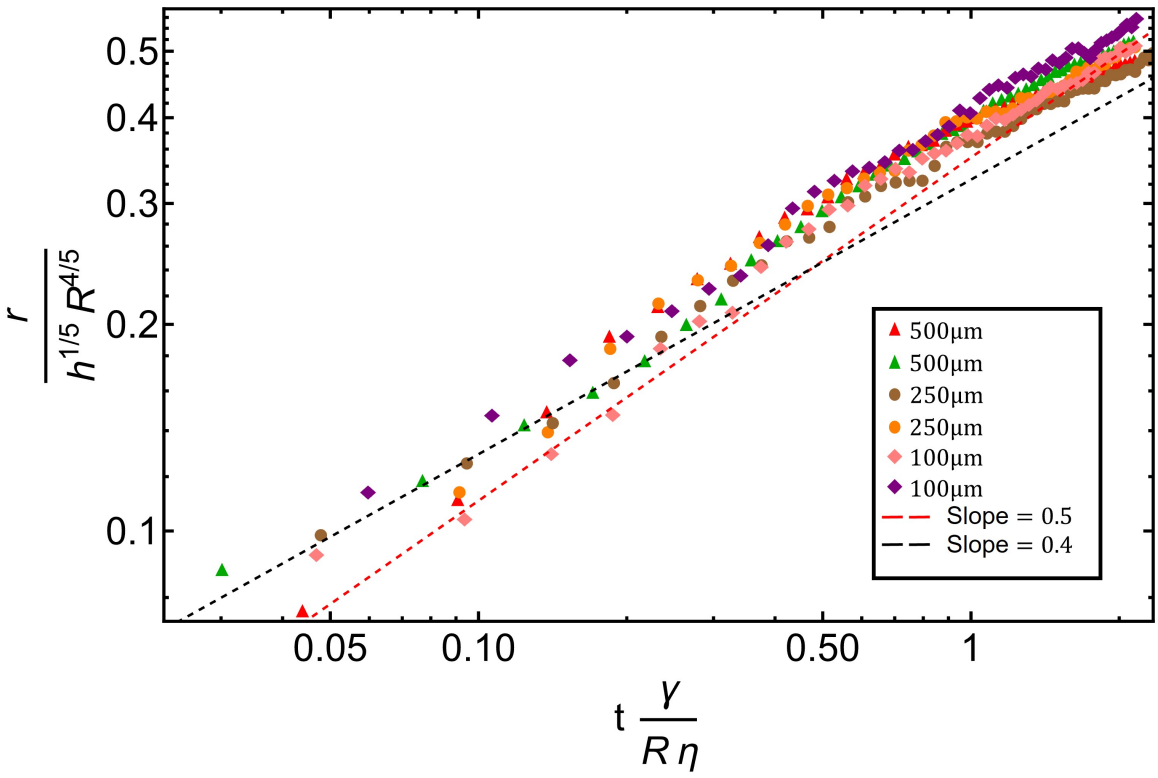

Figure 3.4: Neck width in time plotted after rescaling the horizontal axis by $\frac{R\eta}{\gamma}$ and the vertical axis by $h^{1/5}R^{4/5}$ which was determined empirically. Dotted lines guide the eye to a slope of 0.5 and 0.4

slopes in the collapsed data and noticed that at early times, a power of 1/2 seemed to match the data very well with a cross over to a 0.4 power law after some point. We cannot pinpoint the exact location of this crossover but it is apparent in the data that there must be some crossover. At later times, the 0.4 power law seems to be dominant.

This analysis shows that the fits in Fig. 3.3 are more nuanced since there might be different power laws dominating at different times.

3.3 Measuring curvatures

We know that the curvature of the neck during coalescence is important because it defines a length scale at which flows occur during the process. We try and measure

the curvature of the neck in our experiments using some rudimentary methods.

We import the images of our experiment into Wolfram Mathematica and use those tools to click off points along the edge of the neck as shown in Fig. 3.5. We then create an parametric interpolation from the coordinates of these clicked off points to create the plot as shown in Fig. 3.6. We do this for 11 frames at varying times in the experiment. We can than use the information from these interpolation plots to find the curvature. We use the equation for curvature (κ) of 2D planar curve described by the variables $x(s)$ and $y(s)$.

$$\kappa = \frac{|x'y'' - x''y'|}{((x')^2 + (y')^2)^{3/2}} \tag{3.2}$$

We can then average this curvature around the neck region to obtain a value for the curvature.

We want to see how the curvature changes across the experiment. However, this is not an automated process and would be difficult to execute for all the frames from our experiment. However, we can qualitatively confirm that the curvature decreases through the experiment as seen in Fig. 3.6.

3.4 Variables Comparison

Similar to the analysis in Fig. 1.4 we plotted the various length scales in our experiment on a log number plot. In our experiment, the neck width is always larger than the gap size. However, because of the arresting of the coalescence, we see that the neck width never exceeds a drop radius.

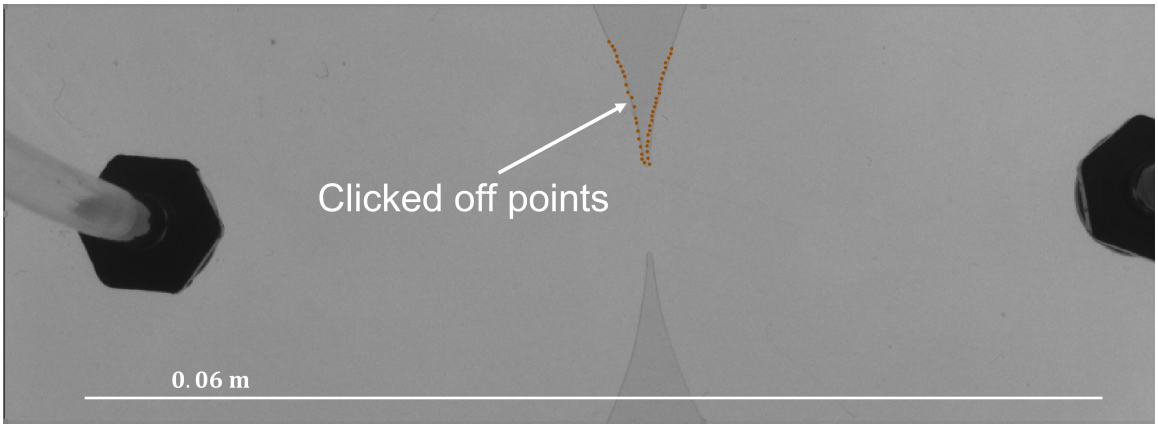

Figure 3.5: Clicking off points in an image from our experiment to extract the curvature of the neck. Orange points are the points used to extrapolate the curvature.

We note that that in our experiment, the gap size is not the smallest length scale. The radius associated with the curvature, given by r^2/R is an order smaller than the gap size at early times in the coalescence. However, for later times in the experiment we see that this length scale is comparable and an order larger than the gap size. This means that we cannot conclude that our experiment is in the Darcy flow regime for the entire experiment. However, if our coalescence did not arrest, we could be approaching the region where Darcy flow becomes the governing law. In order to capture both early and late behaviour in Darcy flow regime, we would have to make the gap size smaller by at least an order. This poses a large experimental challenge.

However, even though we are not in Darcy flow regime, why do we not see a similar power law scaling like in Ref. [4] and Ref. [3]? For one, the length scale comparison of the neck width and drop radius is very different in those studies. Further, our experiment is not under the influence of gravity nor are we dealing with liquid crystal formations and colloidal interactions. Further, we have a large frictional term coming from the difficulty and insufficient pressure to move the contact line beyond a certain point. There must be some decay contribution from pushing the contact line.

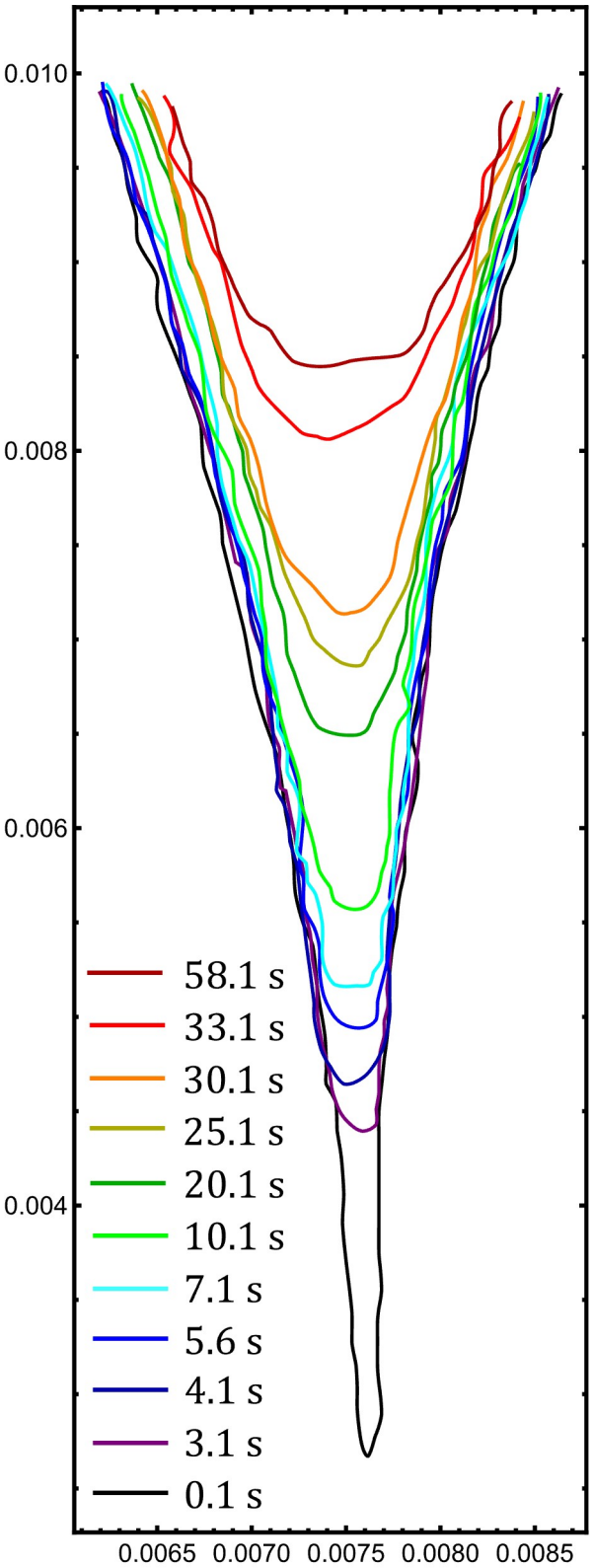

Figure 3.6: Interpolation plots created from clicked off points to qualitatively understand how curvatures evolve in the experiment. Both axes are in metres

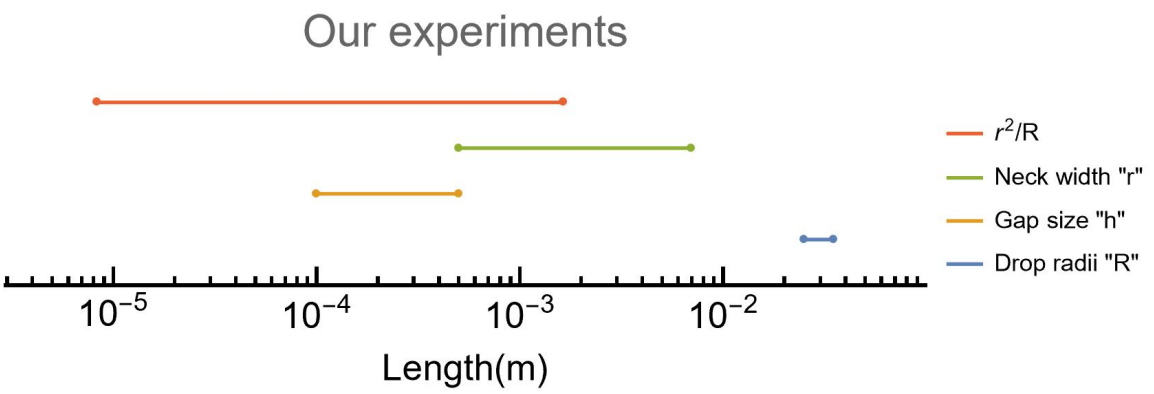

Figure 3.7: Length scales in our experiments plotted on a log number line

3.5 Comparing results to theory

We have established that there are various length scales involved in this story of coalescence and the answer to what is happening is not an easy one. However, we can get a better understanding of what is giving rise to these various power laws from a theoretical perspective established in Yue et. al. and previous works. We will make some simple approximations to understand how we get a power law $r \propto t^{\beta}$. Of course, most of the theory work done is speculative, but we have good reason to believe that there is some accuracy to it and we can make reasonable predictions from it.

Let us first consider what we know. Taking the 3D coalescence of a simple fluid. We know from Ref. [8] and Ref. [2] that the curvature of the neck goes as R^2/r^3, which means that the flows and pressure differences take place at the length scale of r^3/R^2. It is safe to say that the derivatives of the flow and pressure are over this length scale.

Consider the Stokes equation:

$$\boldsymbol{\nabla} P = \eta \nabla^{\mathbf{2}} \mathbf{v} \tag{3.3}$$

The pressure must go as $P \sim \gamma/L$ where is the length scale we picked as r^3/R^2. So we get

$$\eta \frac{\dot{r}}{L^2} \sim \frac{\gamma/L}{L} \Rightarrow \eta \dot{r} \sim \gamma \tag{3.4}$$

And so we get a power law for r where $\beta = 1$. This is as we expect and can see in Fig. 1.2 d)

Let us now consider pure Darcy flow. From Fig. 1.2 we see that curvature goes as R/r^2 and so the length scale over which flows and derivatives of flows take place is r^2/R. So when you consider Darcy's Law

$$\boldsymbol{\nabla} P = -\alpha \mathbf{v} \tag{3.5}$$

The pressure must go as $P \sim \gamma/L$ which in this case gives

$$\dot{r} \sim \frac{\gamma/L}{L} \Rightarrow \dot{r} \sim \frac{\gamma R^2}{r^4} \tag{3.6}$$

And so in this case we get a power law for r where $\beta = 1/5$. This agrees with simulation work done and shown in Fig. 1.2 d)

Let us apply this argument in our case, where we are trying to create a Darcy flow regime, but are getting something in between. We know that $\dot{r} \sim \frac{\gamma}{L^2}$. We can choose L to be various length scales. If we say the flow is along the length r, we get a power law with $\beta = 1/3$. If we chose $L = h$, we get a power law with $\beta = 1$.We can also choose some intermediate where $L^2 = r \times h$ and we get a power law with $\beta = 1/2$. It is possible that our experiments are in this intermediate phase where Darcy flow is not fully applicable.

3.6 Future line of work

There are a few tweaks one can make to this experiment to make it closer to testing Darcy flow. We highlighted that going to smaller gap sizes is quite a challenge. We can decrease the drop size which would make the length scale associated with the curvature much larger. We could also solve the contact line pushing issue with a better substrate. For example, we could do the experiment on glass plates instead because silicone oil wets glass much better than acrylic. This would allow the coalescence process to go much further allowing us to measure larger neck widths putting us in a regime where Darcy flow is the governing law.

Conclusion

Over the last year, we have devised an experiment that can test dynamics of confined droplet coalescence, specifically in a Hele-Shaw cell. We are able to measure the scaling laws and observe the overall shape of this coalescence process. However, as we have shown, it is incredibly challenging to observe coalescence in the Darcy flow regime. There are many length scales that show up in our experiment that are much smaller than the gap size. We have shown that because of this, we cannot consider our experiment to be in Darcy flow. Similarly, past experiments also cannot be considered in Darcy flow regime. In the experiment in Ref. [3], the drop radii are comparable to the gap size which makes the length scales involved more complicated since the gap size is comparable to all the relecant length scales. In Ref. [4], the gap size is comparable to all the length scales in the problem, again making it complicated to understand what the dynamics are and at what length scale the flows are occurring. Further, neither work makes an argument using Darcy's Law and also does not agree with the theoretical work done by Yue et. al.

Our experiments however are in a regime where only the curvature length scale is comparable to the gap size except later in the experiment. However, our experiment involves more complexities with the issue of contact lines. But we can say that our experiment in early times are in agreement with the theoretical work. In the work done by Yue et. al, the initial growth of the neck is given by a power law of 1/2

because a particle width is cutting off any other length scale to impact the result. In our experiment, we claim that the gap size is cutting off these dynamics at early stages.

A lot more work needs to be done to understand the nuances of what length scales are at play. However, we have begun to bridge the gap in our understanding of confined droplet coalescence and how we can use these continuous theory analogs to understand the coalescence dynamics of biological aggregates and colloidal systems.

Bibliography

[1] Ted Frankiewicz and John M. Walsh. The savvy separator: Physical processes behind oil droplet coalescence during water treatment, Jan 2021.

[2] Haicen Yue, Justin C. Burton, and Daniel M. Sussman. Coalescing clusters unveil new regimes of frictional fluid mechanics, 2022. URL https://arxiv.org/abs/2210.06675.

[3] P. V. Dolganov, A. S. Zverev, K. D. Baklanova, and V. K. Dolganov. Dynamics of capillary coalescence and breakup: Quasi-two-dimensional nematic and isotropic droplets. *Phys. Rev. E*, 104:014702, Jul 2021. doi: 10.1103/PhysRevE.104.014702. URL https://link.aps.org/doi/10.1103/PhysRevE.104.014702.

[4] Maria Yokota and Ko Okumura. Dimensional crossover in the coalescence dynamics of viscous drops confined in between two plates. *Proceedings of the National Academy of Sciences*, 108(16):6395–6398, 2011. doi: 10.1073/pnas.1017112108. URL https://www.pnas.org/doi/abs/10.1073/pnas.1017112108.

[5] Joseph D. Paulsen. Approach and coalescence of liquid drops in air. *Phys. Rev. E*, 88:063010, Dec 2013. doi: 10.1103/PhysRevE.88.063010. URL https://link.aps.org/doi/10.1103/PhysRevE.88.063010.

[6] Joseph D. Paulsen, Justin C. Burton, Sidney R. Nagel, Santosh Appathurai, Michael T. Harris, and Osman A. Basaran. The inexorable resistance of inertia

determines the initial regime of drop coalescence. *Proceedings of the National Academy of Sciences*, 109(18):6857–6861, 2012. doi: 10.1073/pnas.1120775109. URL https://www.pnas.org/doi/abs/10.1073/pnas.1120775109.

[7] Joseph D. Paulsen, Justin C. Burton, and Sidney R. Nagel. Viscous to inertial crossover in liquid drop coalescence. *Phys. Rev. Lett.*, 106:114501, Mar 2011. doi: 10.1103/PhysRevLett.106.114501. URL https://link.aps.org/doi/10.1103/PhysRevLett.106.114501.

[8] JENS EGGERS, JOHN R. LISTER, and HOWARD A. STONE. Coalescence of liquid drops. *Journal of Fluid Mechanics*, 401:293–310, 1999. doi: 10.1017/S002211209900662X.

[9] Robert W. Hopper. Coalescence of two viscous cylinders by capillarity: Part i, theory. *Journal of the American Ceramic Society*, 76(12): 2947–2952, 1993. doi: https://doi.org/10.1111/j.1151-2916.1993.tb06594.x. URL https://ceramics.onlinelibrary.wiley.com/doi/abs/10.1111/j.1151-2916.1993.tb06594.x.

[10] Robert W. Hopper. Coalescence of two viscous cylinders by capillarity: Part ii, shape evolution. *Journal of the American Ceramic Society*, 76 (12):2953–2960, 1993. doi: https://doi.org/10.1111/j.1151-2916.1993.tb06595.x. URL https://ceramics.onlinelibrary.wiley.com/doi/abs/10.1111/j.1151-2916.1993.tb06595.x.

[11] Chen Tan and David Julian McClements. Application of advanced emulsion technology in the food industry: A review and critical evaluation. *Foods*, 10(4), 2021. ISSN 2304-8158. doi: 10.3390/foods10040812. URL https://www.mdpi.com/2304-8158/10/4/812.

[12] M. Nasri. Chapter four - protein hydrolysates and biopeptides: Production,

biological activities, and applications in foods and health benefits. a review. volume 81 of *Advances in Food and Nutrition Research*, pages 109–159. Academic Press, 2017. doi: https://doi.org/10.1016/bs.afnr.2016.10.003. URL https://www.sciencedirect.com/science/article/pii/S1043452616300572.

[13] A. Saboni, C. Gourdon, and A.K. Chesters. Drainage and rupture of partially mobile films during coalescence in liquid-liquid systems under a constant interaction force. *Journal of Colloid and Interface Science*, 175(1):27–35, 1995. ISSN 0021-9797. doi: https://doi.org/10.1006/jcis.1995.1425. URL https://www.sciencedirect.com/science/article/pii/S0021979785714257.

[14] Mathias Nagel, Theo A. Tervoort, and Jan Vermant. From drop-shape analysis to stress-fitting elastometry. *Advances in Colloid and Interface Science*, 247:33–51, 2017. ISSN 0001-8686. doi: https://doi.org/10.1016/j.cis.2017.07.008. URL https://www.sciencedirect.com/science/article/pii/S0001868617302701. Dominique Langevin Festschrift: Four Decades Opening Gates in Colloid and Interface Science.

[15] D. Weaire, R. Höhler, and S. Hutzler. Bubble-bubble interactions in a 2d foam, close to the wet limit. *Advances in Colloid and Interface Science*, 247:491–495, 2017. ISSN 0001-8686. doi: https://doi.org/10.1016/j.cis.2017.07.004. URL https://www.sciencedirect.com/science/article/pii/S000186861730204X. Dominique Langevin Festschrift: Four Decades Opening Gates in Colloid and Interface Science.

[16] R. Miller, E.V. Aksenenko, and V.B. Fainerman. Dynamic interfacial tension of surfactant solutions. *Advances in Colloid and Interface Science*, 247:115–129, 2017. ISSN 0001-8686. doi: https://doi.org/10.1016/j.cis.2016.12.007. URL https://www.sciencedirect.com/science/article/pii/

S0001868616303062. Dominique Langevin Festschrift: Four Decades Opening Gates in Colloid and Interface Science.

[17] Zhiwen Zhu, Xing Song, Yiqi Cao, Bing Chen, Kenneth Lee, and Baiyu Zhang. Recent advancement in the development of new dispersants as oil spill treating agents. *Current Opinion in Chemical Engineering*, 36:100770, 2022. ISSN 2211-3398. doi: https://doi.org/10.1016/j.coche.2021.100770. URL https://www.sciencedirect.com/science/article/pii/S2211339821001027.

[18] Sartor and J. Doyne. Electricity and rain. *Physics Today*, 22(8):45–51, 1969. doi: 10.1063/1.3035737. URL https://doi.org/10.1063/1.3035737.

[19] Steffen Grosser, Jürgen Lippoldt, Linda Oswald, Matthias Merkel, Daniel M. Sussman, Frédéric Renner, Pablo Gottheil, Erik W. Morawetz, Thomas Fuhs, Xiaofan Xie, Steve Pawlizak, Anatol W. Fritsch, Benjamin Wolf, Lars-Christian Horn, Susanne Briest, Bahriye Aktas, M. Lisa Manning, and Josef A. Käs. Cell and nucleus shape as an indicator of tissue fluidity in carcinoma. *Phys. Rev. X*, 11:011033, Feb 2021. doi: 10.1103/PhysRevX.11.011033. URL https://link.aps.org/doi/10.1103/PhysRevX.11.011033.

[20] Nastasia V Kosheleva, Yuri M Efremov, Boris S Shavkuta, Irina M Zurina, Deying Zhang, Yuanyuan Zhang, Nikita V Minaev, Anastasiya A Gorkun, Shicheng Wei, Anastasia I Shpichka, et al. Cell spheroid fusion: beyond liquid drops model. *Scientific reports*, 10(1):1–15, 2020.

[21] David Oriola, Miquel Marin-Riera, Kerim Anlaş, Nicola Gritti, Marina Sanaki-Matsumiya, Germaine Aalderink, Miki Ebisuya, James Sharpe, and Vikas Trivedi. Arrested coalescence of multicellular aggregates. *Soft Matter*, 18:3771–3780, 2022. doi: 10.1039/D2SM00063F. URL http://dx.doi.org/10.1039/D2SM00063F.

[22] Stephen Mazur and Donald J. Plazek. Viscoelastic effects in the coalescence of polymer particles. *Progress in Organic Coatings*, 24(1):225–236, 1994. ISSN 0300-9440. doi: https://doi.org/10.1016/0033-0655(94)85016-X. URL `https://www.sciencedirect.com/science/article/pii/003306559485016X`.

[23] Christina M. Caragine, Shannon C. Haley, and Alexandra Zidovska. Surface fluctuations and coalescence of nucleolar droplets in the human cell nucleus. *Phys. Rev. Lett.*, 121:148101, Oct 2018. doi: 10.1103/PhysRevLett.121.148101. URL `https://link.aps.org/doi/10.1103/PhysRevLett.121.148101`.

[24] Maria Yokota and Ko Okumura. Coalescence dynamics of a quasi two-dimensional viscous drop. *Journal of the Physical Society of Japan*, 81(Suppl.A): SA015, 2012. doi: 10.1143/JPSJS.81SA.SA015. URL `https://doi.org/10.1143/JPSJS.81SA.SA015`.

[25] Anna Wang, Ryan McGorty, David M. Kaz, and Vinothan N. Manoharan. Contact-line pinning controls how quickly colloidal particles equilibrate with liquid interfaces. *Soft Matter*, 12:8958–8967, 2016. doi: 10.1039/C6SM01690A. URL `http://dx.doi.org/10.1039/C6SM01690A`.